

Pulsed ^{81}Br Nuclear Quadrupole Resonance Spectroscopy of Brominated Flame Retardants and Associated Polymer Blends

Anthony A. Mrse, Youngil Lee, Pamela L. Bryant, Frank R. Fronczek, and Leslie G. Butler*

Department of Chemistry, Louisiana State University, Baton Rouge, Louisiana 70803

Larry S. Simeral*

Albemarle Corporation, P.O. Box 14799, Baton Rouge, Louisiana 70898

Received September 29, 1997. Revised Manuscript Received February 20, 1998

The dispersion of brominated flame retardants in polymers is monitored with ^{81}Br nuclear quadrupole resonance (NQR) using a pulse NQR spectrometer. The NQR spectrometer consists of a homemade 10–300 MHz single-channel NMR console coupled to a broadly tunable probe. The probe is a loop-gap resonator usable from 220 to 300 MHz and is automatically tuned over any 5 MHz region with a stepping motor and a radio frequency bidirectional coupler. ^{81}Br NQR spectra of several brominated aromatic flame retardants, as pure materials and in polymers, were recorded in the range of 227 to 256 MHz in zero applied magnetic field. Two factors affect the $^{79/81}\text{Br}$ NQR transition frequencies in brominated aromatics: electron-withdrawing substituents on the ring and intermolecular contacts with other bromine atoms in the crystal structure. An existing model for substituents is updated, and a point charge model for the intermolecular contacts is developed. In this study, we exploit the ^{81}Br NQR transition frequency dependence on intermolecular contacts to learn how a flame retardant is dispersed in a polymer matrix. Additionally, the crystal structure for 1-bromo-4-(4-bromophenoxy)benzene and the 100 K structure of 1,2,4,5-tetrabromobenzene were determined.

Introduction

High-impact polystyrene (HIPS) is widely used in consumer products and can be made less flammable with the addition of flame retardants, generally halogenated hydrocarbons or aromatics. To better understand these flame retardant/polymer blends, it is necessary to have an understanding of their structure at a molecular level. The solubilization of flame retardants in HIPS has been studied using thermal optical analysis (TOA) by Spenkle et al.¹ 1-(2,3,4,5,6-pentabromophenoxy)-2,3,4,5,6-pentabromobenzene was found to be soluble, and its solubilization was examined as a function of thermal history. A more recent investigation by Radloff et al. using the techniques of ^1H and ^{13}C solid-state NMR spectroscopy, differential scanning calorimetry, X-ray scattering, and dynamic mechanical analysis yielded the following results: 1-(2,3,4,5,6-pentabromophenoxy)-2,3,4,5,6-pentabromobenzene is miscible, whereas 3,3',4,4',5,5',6,6'-octabromo-*N,N*-ethylenedipthalimide exists in the HIPS matrix as a microcrystalline phase.² The conclusion was based primarily on X-ray scattering data. Given the problems detecting the crystalline phase of small particles with X-ray scattering, an alternative spectroscopic technique is desired.

In this work, we explore ^{81}Br nuclear quadrupole resonance (NQR) spectroscopy of the bromine sites to study the issue of flame retardant dissolution in polymers.

Bromine NQR poses many challenges, most notably, the very wide frequency range over which transitions may occur; for brominated aromatics, transitions are known from 221.86 to 255.55 MHz for 4-bromoaniline and hexabromobenzene, respectively.^{3,4} A correlation between ^{81}Br transition frequency and aromatic ring substitution was pioneered by Bray³ and is further developed in this work. Hammett σ parameters are used to predict the ^{81}Br NQR transition frequency of the flame retardants to an accuracy of ± 1.6 MHz. A minor difficulty is the lack of published σ values for ortho substitutions. For the heavily substituted aromatic ring systems studied herein, ortho Hammett σ values were generated to best model the ^{81}Br NQR data. An additional effect on the ^{81}Br NQR transition frequency comes from intermolecular contacts, especially bromine–bromine contacts. We use a point charge model to account for these frequency shifts, which can be as large as 2.5 MHz.

The acquisition of NMR or NQR transitions in the range of 220 to 260 MHz is difficult with commercial

(1) Spenkle, W. E.; Southern, J. H. *J. Appl. Polym. Sci.* **1981**, *26*, 2229–38.

(2) Radloff, D.; Spiess, H. W.; Books, J. T.; Dowling, K. C. *J. Appl. Polym. Sci.* **1996**, *60*, 715–20.

(3) Bray, P. J.; Barnes, R. G. *J. Chem. Phys.* **1954**, *22*, 2023–5.

(4) Cassabella, P. A.; Bray, P. J.; Segel, S. L.; Barnes, R. G. *J. Chem. Phys.* **1956**, *25*, 1280–1.

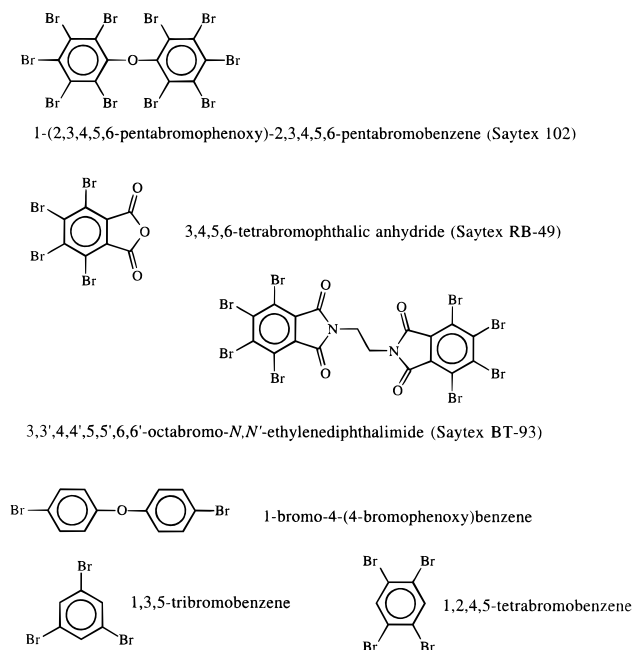


Figure 1. Structures of selected flame retardants and related compounds.

NMR spectrometers. This spectral region is above the ^{31}P NMR resonance for most systems, and the ^1H channel of mid-field spectrometers have limited spectral ranges. Herein, we use a homemade 10–300 MHz NMR spectrometer and an automatically tuned loop-gap resonator probe built for this project.

Herein, we report NQR results for five different brominated aromatic compounds and their associated polymer blends (Figure 1): 1-(2,3,4,5,6-pentabromophenoxy)-2,3,4,5,6-pentabromobenzene (SAYTEX-102; mp 304 °C); 3,3',4,4',5,5',6,6'-octabromo-*N,N'*-ethylenedipthalimide (SAYTEX BT-93; mp 450–455 °C); 1-bromo-4-(4-bromophenoxy)benzene (mp 61–63 °C); 3,4,5,6-tetrabromophthalic anhydride (SAYTEX RB-49; mp 276–282 °C); and 1,3,5-tribromobenzene (mp 121–124 °C).

Theory

Nuclear quadrupole resonance spectroscopy uses instrumentation and techniques similar to NMR spectroscopy to probe the electronic environment near a quadrupolar nucleus. The nuclear electric quadrupole moment, Q , of an $I \geq 1$ nucleus can interact with the electronic environment near that nucleus to affect the nuclear spin angular momentum energy levels, even in zero magnetic field.^{5–7}

$$H_Q = \frac{e^2 q_{zz} Q}{4I(2I-1)} [(3I_z^2 - I^2) + \eta(I_x^2 + I_y^2)] \quad (1)$$

The quantity $e^2 q_{zz} Q/h$ is the quadrupole coupling constant; it is the product of the nuclear electric quadrupole moment and the magnitude of the electric field gradient tensor, represented as q_{zz} . The electric field gradient

tensor is a traceless second-rank tensor fully described in its principal axis system by q_{zz} and η , the asymmetry parameter. The principal axis system is defined by the convention:

$$|q_{zz}| \geq |q_{yy}| \geq |q_{xx}| \quad (2)$$

In this axis system, the asymmetry parameter is defined as

$$\eta = \frac{q_{xx} - q_{yy}}{q_{zz}}; \quad 0 \leq \eta \leq 1 \quad (3)$$

The values of nuclear electric quadrupole moments have been recently reviewed by Pykkö; $Q(^{81}\text{Br}) = 2.76(4) \times 10^{-29} \text{ m}^2$, and the ratio $Q(^{79}\text{Br})/Q(^{81}\text{Br})$ is 1.19705.^{8–10} The parameter $e^2 q_{zz} Q/h$ varies widely for ^{81}Br : near zero for KBr(s) to 731.030(1) MHz for $^{81}\text{BrCl(g)}$.^{10,11} Equation 1 can be solved to yield

$$\nu(|\pm 1/2\rangle \rightarrow |\pm 3/2\rangle) = \frac{e^2 q_{zz} Q}{2h} (1 + \eta^2/3) \quad (4)$$

Because of the near cylindrical symmetry of carbon–bromine bonds, the asymmetry parameter at bromine sites in organic molecules is near zero; thus, the principal axis system for the bromine electric field gradient in C–Br sites has the z -axis aligned with the C–Br bond.^{7,12,13} This alignment was verified using the crystal structure coordinates for 1-bromo-4-(4-bromophenoxy)benzene and the previously reported electric field gradient direction cosine tensor obtained from a Zeeman-perturbed NQR experiment on a single crystal.¹³ Comparison of the Euler rotation angles show the electric field gradient z -axis to be aligned with the C–Br bond to within 3°. The observed ^{81}Br NQR transition frequencies in brominated aromatics range between 220 and 260 MHz.^{3,4} The corresponding ^{79}Br transitions are at slightly higher frequencies as determined by the ratio of the nuclear electric quadrupole moments, $Q(^{79}\text{Br})/Q(^{81}\text{Br})$. The relative natural abundances of bromine nuclei are 50.54% (^{79}Br) and 49.46% (^{81}Br).

^{81}Br NQR transition frequencies can be partially correlated with molecular structure. In addition, there are small frequency shifts that can be attributed to lattice packing. For brominated aromatics, the molecular correlation is accomplished using the Hammett σ parameter of the aromatic ring substituents.³ Aromatic ring substituents alter the charge distribution in the C–Br bond, resulting in a change in the electric field gradient of the bromine site, thereby shifting the bromine transition frequency. The shifts in ^{81}Br transition frequencies for C–Br sites in partially substituted aromatic rings are modeled well with a linear Hammett

(8) Pykkö, P. *Z. Naturforsch A* **1992**, *47*, 189–92.

(9) Pykkö, P.; Li, J.; Pykkö, P.; Li, J. Nuclear Quadrupole Moments. Report HUK1, 1-92, ISSN 0784-0365 1992.

(10) Fowler, P. W.; Legon, A. C.; Peebles, S. A.; Steiner, E. *Chem. Phys. Lett.* **1995**, *238*, 163–7.

(11) Frye, J. S.; Maciel, G. E. *J. Magn. Reson.* **1982**, *48*, 125–31.

(12) Ambrosetti, R.; Angelone, R.; Cecchi, P.; Colligiani, A. *J. Chem. Phys.* **1971**, *54*, 2915–17.

(13) Ambrosetti, R.; Angelone, R.; Colligiani, A.; Cecchi, P. *Mol. Phys.* **1974**, *28*, 551–8.

(5) Gerstein, B. R.; Dybowski, C. R. *Transient Techniques in NMR of Solids*; Academic Press: New York, 1985.

(6) Poole, C. P., Jr.; Farach, H. A. *Theory of Magnetic Resonance*, 2nd ed.; John Wiley: New York, 1987.

(7) Butler, L. G.; Keiter, E. A. *J. Coord. Chem.* **1994**, *32*, 121–34.

relationship:

$$\nu(^{81}\text{Br}) = A + B \sum_i \sigma_i \quad (5)$$

Here, we use literature values for meta and para Hammett σ parameters.^{14,15} The ortho Hammett σ parameters are not generally available. For this reason, we have derived ortho Hammett σ parameters from the ⁸¹Br NQR data by a global minimization (downhill Simplex) of eq 5 for the following substituents: Br, OR, and C(O)R.¹⁶

The crystal structure creates detectable shifts in the ⁸¹Br NQR transition frequencies. For example, three peaks are observed for 1,3,5-tribromobenzene, whereas only one is expected based on molecular symmetry. The crystal structure of 1,3,5-tribromobenzene shows a single molecule in the asymmetric unit with three symmetry-unrelated bromine sites.¹⁷ The three bromine sites on each molecule have significantly different intermolecular Br \cdots Br contacts; the shortest for each site ranging from $d(\text{Br}\cdots\text{Br}) = 3.762$ to 3.859 Å. Neighboring bromine sites can affect the electric field gradient at a given C–Br site.^{18,19} Analogous through-space effects have been observed in solid-state deuterium NMR, and in fact, a Karplus-type relationship was derived based on observed shifts in the deuterium quadrupole coupling constant due to a neighboring oxygen site.²⁰ At first glance, it is surprising that neutral atoms can create an electric field gradient in their vicinity. However, considering the averaging properties of the $1/r^3$ operator for the electric field gradient, one sees that nuclear and electronic terms do not cancel at sites near an atom of high atomic number.

The shifts in ⁸¹Br NQR transition frequencies due to crystal structure effects are conveniently simulated by a point charge model,²¹ where the change in electric field gradient along the z -axis (aligned with the C–Br bond) is given in atomic units by

$$\Delta q_{zz} = K(1 - \gamma_\infty) \sum_i (3 \cos^2(\theta_i) - 1)/r_i^3 \quad (6)$$

and where r_i is the intermolecular Br \cdots Br distance (atomic units, au), θ_i the angle between the z -axis and the vector describing the Br \cdots Br intermolecular contact, and K is a fitted parameter with units of charge (au). In the presence of a point charge, the bromine valence and core orbitals are polarized, and this affects the electric field gradient at the bromine nucleus. A correction term for the point charge model takes the form of $(1 - \gamma_\infty)$ and the best available value for bromine is $\gamma_\infty = -123.0$.²² The summation is truncated to include only Br \cdots Br intermolecular contacts in the first coordi-

ination sphere, i.e., $d(\text{Br}\cdots\text{Br}) \leq 4.5$ Å; there are other possible truncation limits, as discussed by Zax.²³ The conversion factor from atomic units to frequency is^{10,21}

$$\Delta\nu(^{81}\text{Br}) = \Delta q_{zz} \left(\frac{e^2 Q}{4\pi\epsilon_0 a_0^3 h} \right) = \Delta q_{zz} \times 65.76 \text{ MHz au}^{-1} [^{81}\text{Br}] \quad (7)$$

In frequency units, the model predicts frequency shifts of up to 2.5 MHz for $K = -0.0559$ au. This model will be used to assess static line widths in the polymer blends.

In summary, the ⁸¹Br NQR transition frequencies are modeled as a sum of intramolecular (eq 5) and intermolecular effects (eqs 6 and 7). For a brominated aromatic site, the base ⁸¹Br NQR frequency is 226.708 MHz. Substituents on the aromatic ring are observed to cause shifts over a range of 34 MHz, and lattice effects can lead to multiple resonances for chemically similar sites.

Experimental Section

With the exception of 1,3,5-tribromobenzene and 1,2,4,5-tetrabromobenzene (Aldrich), the samples were provided by the Albemarle Corporation: 1-(2,3,4,5,6-pentabromophenoxy)-2,3,4,5,6-pentabromobenzene (SAYTEX-102), 3,4,5,6-tetrabromophthalic anhydride (SAYTEX RB-49), 3,3',4,4',5,5',6,6'-octabromo-*N,N*-ethylenediphthalimide (SAYTEX BT-93), and 1-bromo-4-(4-bromophenoxy)benzene. Powder X-ray diffraction studies were done on all three flame retardants and show that the samples are crystalline, with no evidence for an amorphous component. The powder X-ray diffraction spectrum for 1-(2,3,4,5,6-pentabromophenoxy)-2,3,4,5,6-pentabromobenzene has been reported.² The flame retardant/high-impact polystyrene blends were melt processed at 220 °C;² the blends are 20% by mass brominated aromatic unless otherwise noted. Thermoset polyester blends were prepared with 1,3,5-tribromobenzene and 1-bromo-4-(4-bromophenoxy)benzene and Alpha/Corning Altek 78–70 polyester resin. The brominated aromatics were mechanically stirred into the polyester at the polymerization temperature immediately after the polyester was made. The visual appearance (phase separation into optically clear and cloudy needle-containing domains) of the 1,3,5-tribromobenzene/polyester indicates that this brominated aromatic exists as microcrystalline domains in the polymer matrix, while the very clear and homogeneous appearance of the 1-bromo-4-(4-bromophenoxy)benzene/polymer suggests a stable solution.

^{79/81}Br NQR spectroscopy of the pure brominated aromatics and their polymer blends were performed with a homemade NMR spectrometer and a concentric loop-gap resonator probe.^{24,25} The 10–300 MHz NMR spectrometer includes a Tecmag pulse programmer and the spectrometer is controlled with a Macintosh Centris 650 running a program written in LabVIEW. An American Microwave Technology M3205 pulse amplifier (300 W, 6–220 MHz) is used. The RF gain falloff is rapid near 250 MHz, so the input drive level was adjusted to maintain a constant 45 W RF pulse power for all spectra.

The ⁸¹Br transition frequencies for bromine bound to an aromatic carbon site generally occur in a frequency range of 220–260 MHz, a range which is difficult to cover with most commercial NMR spectrometers (i.e., a Chemagnetics Infinity 400 cannot do this experiment). To scan over the desired

(14) Jaffe, H. H. *Chem. Rev.* **1953**, *53*, 191–261.

(15) Wells, P. R. *Chem. Rev.* **1963**, *63*, 171–219.

(16) Press, W. H.; Flannery, B. P.; Teukolsky, S. A.; Vetterling, W. T. *Numerical Recipes*; Cambridge University Press: Cambridge, 1986.

(17) Milledge, J. H.; Pant, L. M. *Acta Crystallogr.* **1960**, *13*, 285–90.

(18) Ambrosetti, R.; Bucci, P.; Cecchi, P.; Colligiani, A. *J. Chem. Phys.* **1969**, *51*, 852–3.

(19) Bray, P. J.; Barnes, R. G. *J. Chem. Phys.* **1957**, *27*, 551–60.

(20) Jackisch, M. A.; Jarrett, W. L.; Guo, K.; Fronczek, F. R.; Butler, L. G. *J. Am. Chem. Soc.* **1988**, *110*, 343–7.

(21) Wu, X.; Fronczek, F. R.; Butler, L. G. *Inorg. Chem.* **1994**, *33*, 1363–1365.

(22) Sternheimer, R. M. *Phys. Rev.* **1966**, *146*, 140–60.

(23) Chew, B. G. M.; Golden, J. H.; Huggins, B. A.; DiSalvo, F. J.; Zax, D. B. *Phys. Rev. B* **1994**, *50*, 7966–76.

(24) Wu, X.; Patterson, D. A.; Butler, L. G. *Rev. Sci. Instrum.* **1993**, *64*, 1235–8.

(25) Koskinen, M. F.; Metz, K. R. *J. Magn. Reson.* **1992**, *98*, 576–88.

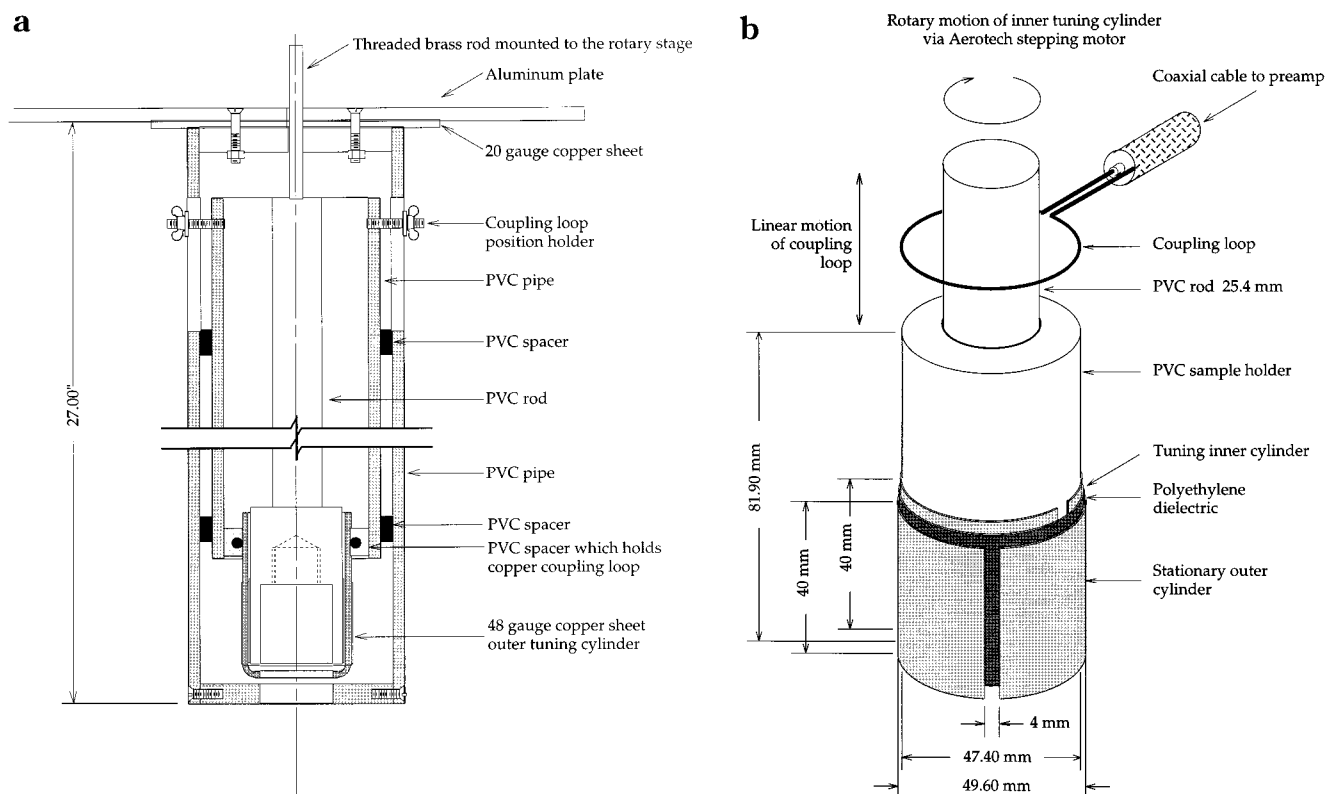


Figure 2. Loop-gap resonator probe (views a and b).

domain, a broadband 210–300 MHz loop-gap resonator probe (Figure 2a) was constructed with the capability of automatic tuning. In a loop-gap resonator probe, current flows through a thin metal sheet arranged in a nearly cylindrical geometry. The current path is broken by a gap in the metal sheet; the edges of the gap form the capacitor of a tuned RF circuit (the resonator). Two or more loop-gaps can be assembled, one inside the other. Tuning is achieved by rotating the relative position of gaps in nested cylinders. The resonator is coupled to the NMR spectrometer by a coupling loop, and impedance matching is accomplished by altering the distance between the coupling loop and the resonator. The resonator is made from copper foil, and the critical dimensions are shown in Figure 2b. The two loop-gaps are separated by a polyethylene sheet while the resonator is mounted on a polyvinyl chloride (PVC) body which is threaded on the inside to accept a 20 mL scintillation vial containing the sample.

The inner conductor is affixed to a PVC shaft connected to a computer-controlled rotary stage. Course automatic frequency tuning is done with the use of a fourth-order polynomial function relating rotary stage position with tuning frequency. Fine-tuning is done with a search algorithm where the probe performance is monitored by observing the forward and reflected power of a $\sim 50 \mu\text{s}$ RF pulse with a bidirectional coupler and a four-channel digital oscilloscope. Impedance matching is done manually. Figure 3 shows overall probe performance. The probe body is long, 69 cm. Before the incorporation of a grounded plate at the midpoint, the probe body resonated at 250 MHz, obscuring NQR signals at this frequency.

The 90° ^{81}Br pulse is $50 \mu\text{s}$ at 230 MHz and 45 W, as measured for 1,3,5-tribromobenzene with a solid echo pulse sequence: $90^\circ(\theta_1) - \tau_1 - 90^\circ(\theta_2) - \tau_2 - A Q(\theta_3)$. The long 90° pulse is ineffective for broad ^{81}Br transitions as found for 3,4,5,6-tetrabromophthalic anhydride/polymer. Thus, the typical pulse sequence was $45^\circ(\theta_1) - \tau_1 - 45^\circ(\theta_2) - \tau_2 - A Q(\theta_3)$ [$\theta_1 = (x, -x, -x, x)$; $\theta_2 = (y, y, -y, -y)$; and $\theta_3 = (x, -x, -x, x)$] with $\tau_1 = 16 \mu\text{s}$ and $\tau_2 = 28 \mu\text{s}$. The ^{81}Br T_2 was measured for 3,4,5,6-tetrabromophthalic anhydride (the resonance at 254.614 MHz) and is $38 \mu\text{s}$. The ^{81}Br spin-lattice relaxation times were not measured, but a recycle delay of 0.4 s does not cause detectable

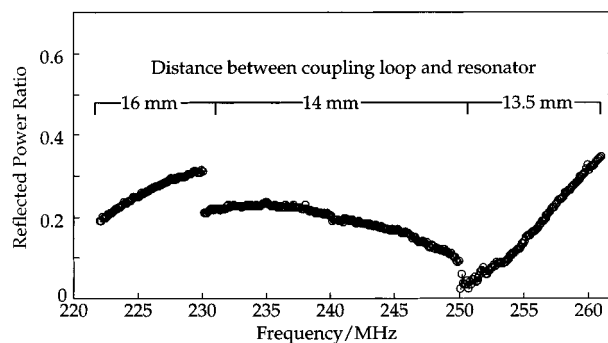


Figure 3. Probe performance. A reflected power of 0.4 or less yielded satisfactory sensitivity; for most runs, the reflected power was about 0.2.

saturation (the minimum recycle delay was determined by the time required for oscilloscope data readout). The spectrum in Figure 4 of a 15 g sample of 1,3,5-tribromobenzene was acquired in 4 h, and the signal at each frequency increment is the average of 400 scans. A typical sweep range is between 3 and 10 MHz, and frequency increments range between 15 and 30 kHz. Sample temperature was monitored before and after each run. The transitions in 1,3,5-tribromobenzene have a temperature coefficient of $-15 \text{ kHz}/^\circ\text{C}$; in 1,2,4,5-tetrabromobenzene, the temperature coefficient is $-14 \text{ kHz}/^\circ\text{C}$.^{3,26} Transition frequencies, line widths, and absorption amplitudes were extracted by fitting the resonances to a Gaussian function with a nonlinear least-squares program; the baseline was modeled with a quadratic function.²⁷

X-ray Experimental, 1-Bromo-4-(4-bromophenoxy)-benzene. Four octants of diffraction data were collected at 25°C on an Enraf-Nonius CAD4 diffractometer equipped with $\text{Mo K}\alpha$ radiation and a graphite monochromator (Table 1). Accurate unit cell parameters were obtained by least-squares

(26) Johnson, F. B. *Nature* **1956**, 178, 590.

(27) Bevington, P. R. *Data Reduction and Error Analysis for the Physical Sciences*; McGraw-Hill: New York, 1969.

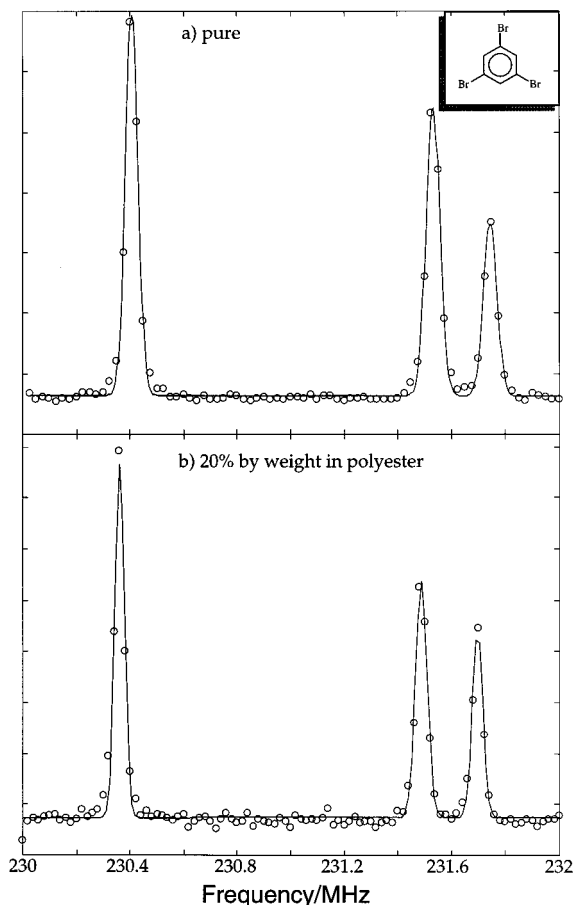


Figure 4. Spectrum of 1,3,5-tribromobenzene, pure and mixed in polyester.

refinement vs $\sin \theta/\lambda$ values for 25 reflections ($9^\circ < \theta < 22^\circ$). Data reduction included corrections for background, Lorentz, and polarization effects and absorption corrections based on ψ scans. Standard reflections indicated no intensity decay during data collection. The structure was solved by heavy-atom methods. Refinement was by full-matrix least-squares, with neutral-atom scattering factors and anomalous dispersion corrections. All non-hydrogen atoms were refined anisotropically, while H atoms were placed in calculated positions. Calculations were carried out using the MolEN programs.²⁸ The absolute structure was determined by refinement of the antipodal structure under identical circumstances, leading to $R = 0.068$, $R_w = 0.071$, $\text{GOF} = 3.106$. Atomic positions of the correct absolute structure are listed in Table 2, and bond distances are given in Table 4.

X-ray Experimental, 1,2,4,5-Tetrabromobenzene. One quadrant of diffraction data was collected at 100 K with an Oxford Cryostream temperature controller (Table 1). Accurate unit cell parameters were obtained by least-squares refinement vs $\sin \theta/\lambda$ values for 25 reflections ($18^\circ < \theta < 24^\circ$). Data reduction included corrections for background, Lorentz, and polarization effects and absorption corrections based on ψ scans. Standard reflections indicated no intensity decay during data collection. The structure was solved by heavy-atom methods. Refinement was by full-matrix least-squares, with neutral-atom scattering factors and anomalous dispersion corrections. All non-hydrogen atoms were refined anisotropically, while the H atom was refined isotropically. Atomic positions are listed in Table 3, and bond distances are given in Table 5. A packing diagram is shown in Figure 5.

(28) Fair, C. K., Fair, C. K. MolEN, An Interactive Structure Solution Procedure, Delft, The Netherlands, 1990.

Table 1. Crystal, Experimental, and Refinement Data for 1-Bromo-4-(4-bromophenoxy)benzene and 1,2,4,5-Tetrabromobenzene

mol formula	$\text{C}_{12}\text{H}_8\text{Br}_2\text{O}$	$\text{C}_6\text{H}_2\text{Br}_4$
fw	328.0	393.72
crystal system	orthorhombic	monoclinic
space group	$Ccc2$	$P2_1/n$
temp	298 K	100 K
cell constants		
a , Å	7.6837(10)	3.924(1)
b , Å	26.620(2)	10.4885(8)
c , Å	5.7250(7)	10.367(1)
β , deg		100.37(2)
V , Å ³	1171.0(4)	419.7(2)
Z	4	2
D_{calcd} , g cm ⁻³	1.860	3.116
μ , cm ⁻¹	68.3	189.2
diffractometer/scan	Enraf-Nonius CAD4/ $\omega-2\theta$	$\omega-2\theta$
radiation	Mo K α ($\lambda = 0.71073$ Å)	Mo K α
cryst dimens, mm ³	$0.53 \times 0.32 \times 0.18$	$0.37 \times 0.15 \times 0.15$
color/shape	colorless prism	colorless needle
min rel transmissn, %	37.25	50.32
decay of standards	<1%	1.4
unique reflections	1700	3458
2θ range, deg	$2 < 2\theta < 60$	$2 < 2\theta < 90$
range of h, k, l	-10 to 10 , -37 to 37 , -8 to 8	-7 to 0 , 0 to 20 , -20 to 20
obsd reflcns [$I > 1\sigma(I)$]	877	2234
no. of params refined	69	51
weights	$4F_o^2/[\sigma^2(I) + (0.02F_o^2)^2]^{-1}$	same
$R = \sum \Delta F / \sum F_o $	0.051	0.052
$R_w = (\sum w(\Delta F)^2 / \sum wF_o^2)^{1/2}$	0.047	0.037
GOF	2.082	1.223
max. resid density, e Å ⁻³	0.74	1.51
min. resid density, e Å ⁻³	-0.63	-1.54

Table 2. Coordinates and Equivalent Isotropic Displacement Parameters for 1-Bromo-4-(4-bromophenoxy)benzene

atom	x	y	z	B_{eq} (Å ²) ^a
Br	0.72853(9)	0.54660(2)	1/2	7.19(2)
O1	3/4	3/4	0.962(1)	4.6(1)
C1	0.7485(6)	0.7051(2)	0.8401(9)	3.3(1)
C2	0.8281(7)	0.6646(2)	0.9479(9)	4.2(1)
C3	0.8209(8)	0.6170(2)	0.848(1)	4.3(1)
C4	0.7386(7)	0.6100(3)	0.646(1)	4.4(1)
C5	0.6585(6)	0.6502(2)	0.5342(8)	3.8(1)
C6	0.6634(7)	0.6978(2)	0.631(1)	3.8(1)

$$B_{\text{eq}} = 8\pi^2/3 \sum_i \sum_j U_{ij} a_i^* a_j^* \mathbf{a}_i \cdot \mathbf{a}_j$$

Table 3. Coordinates and Equivalent Isotropic Displacement Parameters for 1,2,4,5-Tetrabromobenzene

atom	x	y	z	B_{eq} (Å ²) ^a
Br1	0.65170(9)	0.20188(3)	0.58692(3)	1.039(5)
Br2	0.39084(9)	0.41519(3)	0.79429(3)	0.985(5)
C1	0.5619(8)	0.3744(3)	0.5392(3)	0.77(5)
C2	0.4559(8)	0.4615(3)	0.6247(3)	0.85(5)
C3	0.3932(8)	0.5879(3)	0.5863(3)	0.93(5)
H3	0.33(1)	0.641(4)	0.645(4)	3(1)

$$^a B_{\text{eq}} = 8\pi^2/3 \sum_i \sum_j U_{ij} a_i^* a_j^* \mathbf{a}_i \cdot \mathbf{a}_j$$

Results

^{81}Br NQR Spectroscopy. ^{81}Br NQR transitions are detected for all pure materials at room temperature. For the pure materials, the ^{81}Br T_1 s are shorter than the recycle delay of the spectrometer, 0.4 s, and the T_2 s were about 40 μs or longer ($T_2 = 38 \mu\text{s}$ for 3,4,5,6-tetrabromophthalic anhydride). Previously, ^{81}Br NQR spectroscopy of brominated organics used self-quenched superregenerative spectrometers.¹⁹ With that technique,

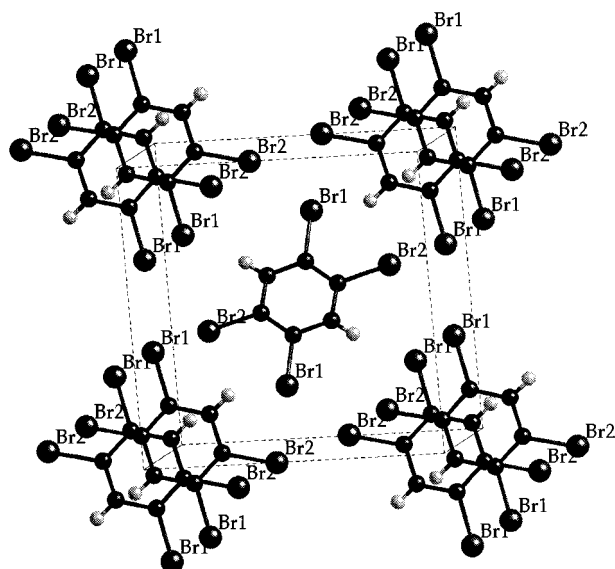


Figure 5. Packing diagram for 1,2,4,5-tetrabromobenzene (100 K).

Table 4. Bond Distances for 1-Bromo-4-(4-bromophenoxy)benzene

atoms	distance (Å)	atoms	distance (Å)
Br C4	1.886(7)	C2 C3	1.393(8)
O1 C1	1.384(6)	C3 C4	1.329(8)
C1 C2	1.385(8)	C4 C5	1.393(8)
C1 C6	1.380(7)	C5 C6	1.383(8)

Table 5. Bond Distances for 1,2,4,5-Tetrabromobenzene

atoms	distance (Å)	atoms	distance (Å)
Br1 C1	1.892(3)	Br2 C2	1.885(3)
C1 C2	1.389(5)	C1 C3	1.401(5)
C3 H3	0.90(5)	C2 C3	1.393(5)

some combinations of T_1 and T_2 make it difficult to detect ^{81}Br NQR transitions at room temperature, hence the reason for performing many of the early ^{81}Br NQR studies at 77 K. The pulsed NQR spectrometer used herein is able to accommodate a wide range of relaxation times. However, as will be shown below, the dissolution of brominated aromatics into a polymer matrix can yield such broad line widths as to make signal detection difficult.

Two spectra of 1,3,5-tribromobenzene, both pure and mixed in polyester, are shown in Figure 4. For the pure material, the scan range of 2 MHz required 4 h. In 1954, Bray and co-workers reported three resonances of 1,3,5-tribromobenzene at room temperature, as observed here, but with some overlap of the two high-frequency resonances due to the super-regenerative oscillator sidebands.³ The crystal structure of 1,3,5-tribromobenzene¹⁷ shows three distinct sites for bromine and is thus consistent with the spectrum. Each peak was fitted to a Gaussian function for the purpose of determining an integrated area. The measured ratio for this spectrum is 1:0.83:0.48, vs the expected ratio of 1:1:1. Also, the ratio of the peak areas is found to vary from run to run. The variation is attributed to differences in probe performance that remain despite the automatic tuning. The integrated peak areas for the blends are therefore regarded as crude measures of ^{81}Br NQR signal strength; however, the peak positions and line widths are well determined.

For the 1,3,5-tribromobenzene/polyester mixture, the ^{81}Br NQR transition frequencies are the same as for the pure brominated aromatic, and the ratio of peak areas is similar. When corrected for the number of scans, the ratio of peak areas of polymer mixture vs pure brominated aromatic is 0.152, near the expected 0.20 for the 20% by mass 1,3,5-tribromobenzene/polyester mixture. Since the crystallographic differences in the bromine sites appear to be retained in the 1,3,5-tribromobenzene/polyester mixture, the ^{81}Br NQR spectrum is taken as evidence that 1,3,5-tribromobenzene has not dissolved in the polyester. Visually, the 1,3,5-tribromobenzene/polyester mixture appears to be a clear polymer matrix with suspended crystallites of 1,3,5-tribromobenzene. To our knowledge, 1,3,5-tribromobenzene is not used as a flame retardant in polymers.

The ^{81}Br NQR spectra of three commercial flame retardants and their high-impact polystyrene blends are shown in Figure 6. Figure 7 shows the ^{81}Br NQR spectra of 1-bromo-4-(4-bromophenoxy)benzene, both the pure and dissolved in polyester. Table 6 summarizes the observed ^{81}Br NQR transition frequencies and line widths. The frequencies of the pure materials were used to help generate the ortho Hammett σ values listed in Table 7. The Hammett σ values for the brominated sites are listed in Table 6, together with the transition frequencies predicted from eq 5 with the fitted parameters: $A = 226.708$ MHz, $B = 5.4766$ MHz. A plot of the correlation between Hammett σ values and observed ^{81}Br NQR transition frequencies is shown in Figure 8.

The correlation given by eq 5 suffices to predict spectral regions for ^{81}Br NQR transitions, but is not sufficient to generally allow the association of a resonance to a specific bromine site. The molecular structure and Hammett σ values for 1-(2,3,4,5,6-pentabromophenoxy)-2,3,4,5,6-pentabromobenzene suggest three peaks over a 1.7 MHz range; two peaks are observed within this range, but separated by only 0.5 MHz (Figure 6a). For 3,4,5,6-tetrabromophthalic anhydride, two peaks are expected separated by 1.6 MHz; four peaks are found over a 1.8 MHz range (Figure 6b). For 3,3',4,4',5,5',6,6'-octabromo-*N,N'*-ethylenedipthalimide, two peaks, separated by 1.7 MHz, are expected, whereas one peak is observed in the midst of this range (Figure 6c). Last, we note that the line widths for the pure flame retardants are between 34 and 214 kHz.

The hierarchy of factors that determined ^{81}Br NQR transition frequencies is as follows: (1) formation of a C-Br bond, with $d(\text{C}-\text{Br})$ of about 1.89 Å, yields a transition frequency of 226.708 MHz (parameter A of eq 5); (2) ring substituents shift the frequency over a range of 34 MHz (eq 5, parameter $B \times \text{range of } \sigma$); and (3) lattice effects shift frequencies by several megahertz. We briefly explored lattice effects by examining the structures and transition frequencies of two symmetric molecules, 1,3,5-tribromobenzene and 1,2,4,5-tetrabromobenzene. The crystal structures are not known for any of the flame retardants. Attempts to grow crystals of a suitable size for X-ray crystallography failed; these materials have very low solubilities in xylene and toluene. The molecular structures of 1,3,5-tribromobenzene and 1,2,4,5-tetrabromobenzene would suggest that each has a single resonance, yet multiple resonances

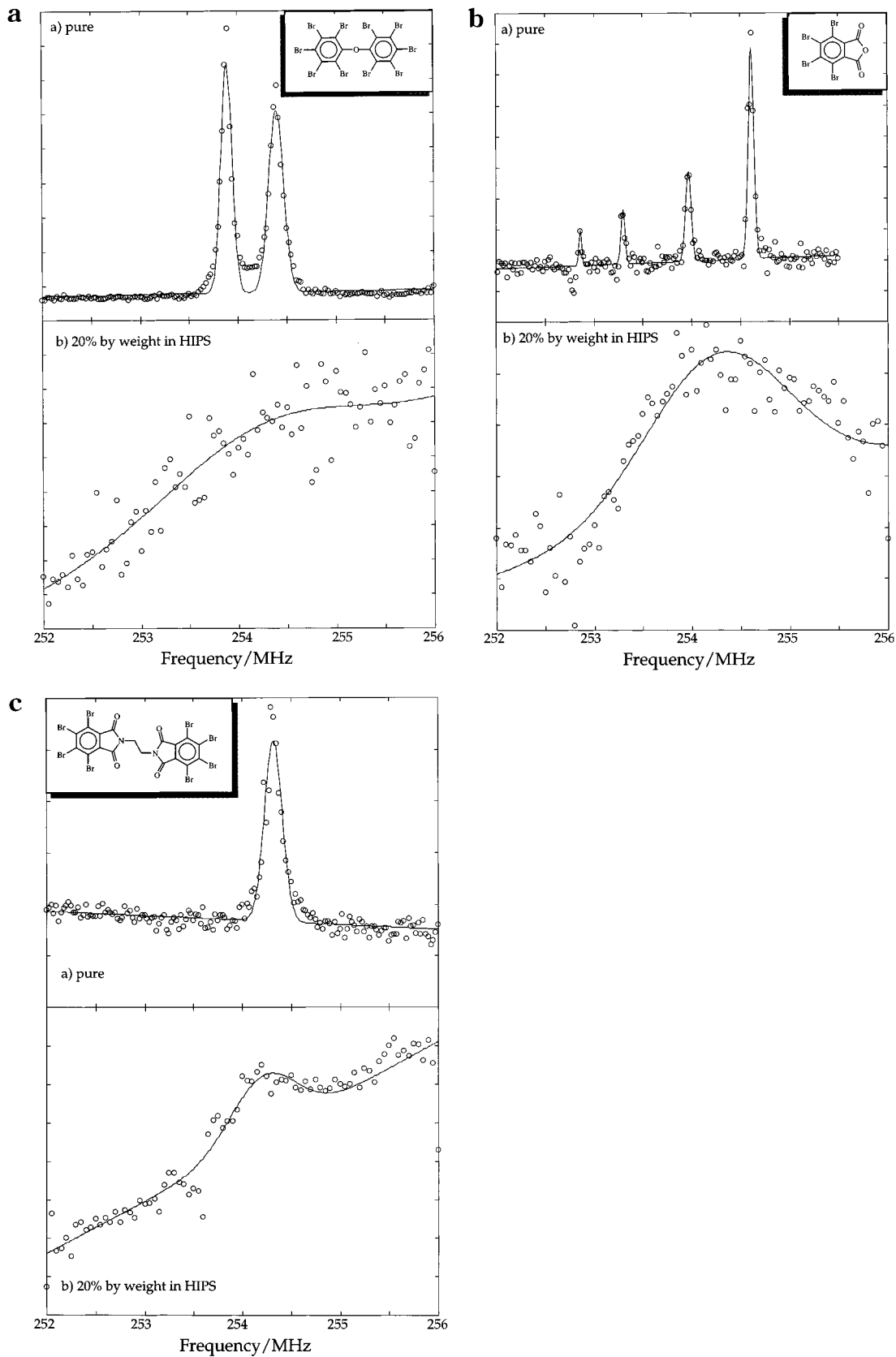


Figure 6. ^{81}Br NQR spectra of three flame retardants (pure and in high impact polystyrene): (a) 1-(2,3,4,5,6-pentabromophenoxy)-2,3,4,5,6-pentabromobenzene (Saytex 102), (b) 3,4,5,6-tetrabromophthalic anhydride (Saytex RB-49), and (c) 3,3',4,4',5,5',6,6'-octabromo-*N,N*-ethylenedipthalimide (Saytex BT-93). The frequency-dependent baselines are a consequence of changes in probe tuning over the scan range (see Figure 3). The weak signals in the HIPS are not easily observed; note the ratios of integrated peak areas from the Gaussian fits as listed in Table 6.

are observed for each (Table 6). The origin of this crystal structure effect is most likely the electron density

associated with neighboring bromine sites. A simple point charge model is chosen to model the frequency

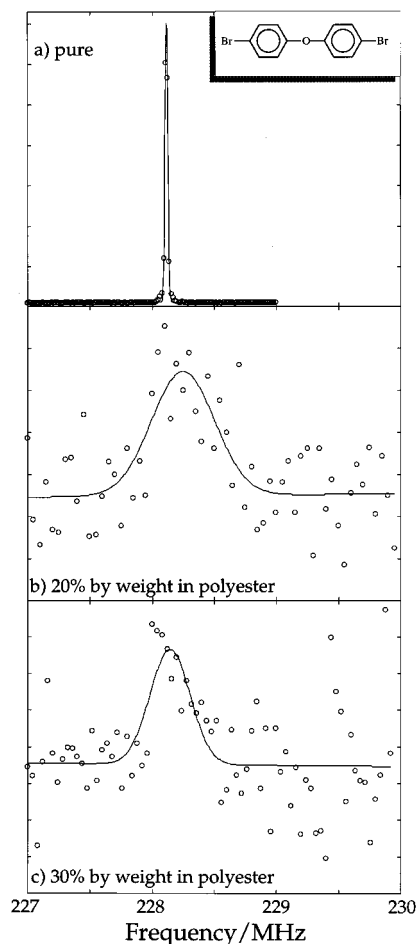


Figure 7. Spectra of 1-bromo-4-(4-bromophenoxy)benzene, pure and dissolved in polyester.

shifts, and the results are shown in Figure 9. From this, we conclude that a distribution of ^{81}Br NQR transition frequencies can be expected from a noncrystalline solid. For a random set of $\text{Br}\cdots\text{Br}$ intermolecular contacts, one would expect a line width on the order of 1–3 MHz.

The ^{81}Br NQR spectra of flame retardants in HIPS are shown in Figure 6. The signal-to-noise ratios for these spectra are extremely low. Since it is known that the samples contain bromine and the anticipated frequency shifts are encompassed by the scan ranges, the very small signals in these spectra are attributed to ^{81}Br NQR transitions. The line widths are the most informative features: For 1-(2,3,4,5,6-pentabromophenoxy)-2,3,4,5,6-pentabromobenzene/HIPS (Figure 6a), the fitted line width is huge, possibly as large as 2 MHz; however, the ^{81}Br NQR absorption is not definitively observed. For 3,4,5,6-tetrabromophthalic anhydride/HIPS (Figure 6b), the line width is 1.7 MHz and is associated with a better-defined absorption. The dramatic difference in line widths of the two pure materials vs line widths of their associated HIPS blends indicates a substantial change in the range of $\text{Br}\cdots\text{Br}$ intermolecular contacts. We assert that this is evidence of flame retardant dissolution in HIPS. As support of this statement, transmission electron microscopy (TEM) images have been used as evidence that both 3,4,5,6-tetrabromophthalic anhydride and octabromodiphenyl

oxide blend with acrylonitrile–butadiene–styrene (ABS).²⁹

The flame retardant 3,3',4,4',5,5',6,6'-octabromo-*N,N*-ethylenedipthalimide in HIPS (Figure 6c) shows a ^{81}Br NQR transition that is substantially broader than for the pure material: 799 kHz vs 214 kHz. This indicates some change in the environment at bromine sites, but less than that noted for the other flame retardants. Interestingly, wide-angle X-ray scattering shows a crystalline component for 3,3',4,4',5,5',6,6'-octabromo-*N,N*-ethylenedipthalimide in HIPS, but scattering only from an amorphous phase for 1-(2,3,4,5,6-pentabromophenoxy)-2,3,4,5,6-pentabromobenzene in HIPS.² Likewise, TEM images of this flame retardant in ABS show particles on the order 0.8 μm , indicating insolubility.²⁹

The lightly brominated aromatic, 1-bromo-4-(4-bromophenoxy)benzene, was studied both as the pure material and in 20 and 30 wt % in polyester. The ^{81}Br NQR spectra (Figure 7) show a dramatic change in line width on going from pure material to dissolution in HIPS, an increase from 27 kHz to about 500 kHz for the very weak ^{81}Br NQR transitions in the blends. On the basis of the point charge model for line widths, it appears that 1-bromo-4-(4-bromophenoxy)benzene is well dispersed in the polyester phase.

The point charge model of eq 7 is used to account for line broadening as a distribution of static sites. An estimate of the effect of a range of $\text{Br}\cdots\text{Br}$ contacts is obtained from an analysis of the symmetric molecules 1,3,5-tribromobenzene and 1,2,4,5-tetrabromobenzene (Figure 9). This plot indicates that contacts can shift ^{81}Br NQR transition frequencies by up to 2.5 MHz, thereby largely accounting for the line widths in the polymer blends. One shortcoming of this analysis is that an amorphous phase consisting only of the brominated compound is also expected to have an exceedingly broad ^{81}Br NQR line width, much as seen for the flame retardants in Figure 6a,b. The supporting evidence of X-ray powder diffraction and TEM images show that the flame retardants studied herein will either dissolve in HIPS or remain as microcrystalline domains; they do not undergo phase changes to amorphous, undissolved domains.

Conclusions

Dispersion of a brominated aromatic in a polymer matrix can be determined by a line width analysis of the ^{81}Br NQR resonances. Dispersion yields NQR resonances inhomogeneously broadened relative to the pure crystalline material by factors of 4- to 20-fold. The ^{81}Br NQR transition frequencies were modeled with a linear Hammett σ parameter model; the base frequency is 226.708 MHz with a total range of 34 MHz. Furthermore, lattice effects can shift transitions by 2.5 MHz. It is the lattice effect that changes upon dissolution of the aromatic flame retardants in the polymer matrix. The lattice effects observed in the ^{81}Br NQR spectrum could be due to either dissolution, as proposed herein, or to a phase change to an amorphous, but undissolved, domain.

(29) Uhlmann, J. G.; Oelberg, J. D.; Sikkema, K. D.; Nelb, R. G. *Plast. Compd.* **1993**, May/June, 38–46.

Table 6. ⁸¹Br NQR Spectral Parameters for Flame Retardants in Polymer Blends and Mixtures^a

compound site	σ	calc freq/MHz	observed freq/MHz	line width/kHz	sample composition	ratio of integrated peak areas
1,3,5-Tribromobenzene						
all	0.782	230.991	230.407(5)	55(2)	crystalline	0.152
			231.533(5)	61(3)	"	
			231.745(5)	59(4)	"	
			230.359(5)	42(1)	20% in polyester	
			231.488(5)	51(3)	"	
231.697(5)	45(4)	"				
1-(2,3,4,5,6-Pentabromophenoxy)-2,3,4,5,6-pentabromobenzene						
2	5.083	254.546	254.396(5)	181(11)	crystalline	
3	4.768	252.820	253.890(5)	136(8)	"	
4	4.79	252.941				
			254.224(450)	2308(1800)	20% in HIPS	0.004
3,4,5,6-Tetrabromophthalic Anhydride						
3	4.947	253.801	252.861(9)	34(18)	crystalline	
4	5.207	255.225	253.298(8)	49(16)	"	
			253.971(5)	68(11)	"	
			254.614(5)	74(5)	"	
			254.261(120)	1737(382)	20% in HIPS	
						10.142
3,3',4,4',5,5',6,6'-Octabromo- <i>N,N</i> -ethylenedipthalimide						
3	4.91	253.598	254.320(6)	214(16)	crystalline	
4	5.223	255.312				
			254.210(116)	799(220)	20% in HIPS	1.854
1-Bromo-4-(4-bromophenoxy)benzene						
4	-0.028	226.555	228.117(5)	28(3)	crystalline	
			228.250(84)	595(215)	20% in polyester	
			228.145(68)	381(170)	30% in polyester	
						0.038
						0.026
1,2,4,5-Tetrabromobenzene						
all	2.674	241.352	239.701(5)	86(3)	crystalline	
			242.00 (77 K, ref 3)		"	
			242.75 (77 K, ref 3)		"	

^a Error limits in parentheses are 95% confidence limits (2 × standard deviation).

Table 7. Selected Hammett σ Parameters

site	σ	ref	site	σ	ref
<i>p</i> -Br	0.265	15	<i>m</i> -COOCH ₃	0.317	15
<i>m</i> -Br	0.391	15	<i>o</i> -COOCH ₃	1.956	<i>d</i>
<i>o</i> -Br	2.018	<i>a</i>	<i>p</i> -COCH ₃	0.516	<i>e</i>
<i>p</i> -OC ₆ H ₅	-0.028	14	<i>p</i> -COC ₆ H ₅	0.459	14
<i>o</i> -OC ₆ H ₅	2.018	<i>b</i>	<i>m</i> -CONH ₂	0.28	14
<i>p</i> -OCH ₃	-0.111	15	<i>o</i> -CONH ₂	1.956	<i>d</i>
<i>m</i> -OCH ₃	0.076	<i>c</i>	<i>p</i> -NH ₂	-0.66	14
<i>p</i> -COOCH ₃	0.463	15	<i>p</i> -COOCH ₃	0.463	15

^a Best fit to NQR data. ^b *o*-OC₆H₅ is assigned the same σ value as *o*-Br because of the similar NQR frequencies that are observed for this site. ^c In the absence of a literature value for *m*-OC₆H₅, the value for *m*-OCH₃ is used.¹⁵ ^d *o*-COOCH₃ and *o*-CONH₂ are assumed to be the same and are the best fit to the NQR data. ^e In the absence of a literature value for *p*-CONH₂, the value for *p*-COCH₃ is used.¹⁴

On the basis of dramatically broadened line widths, the brominated aromatics 1-(2,3,4,5,6-pentabromophenoxy)-2,3,4,5,6-pentabromobenzene (SAYTEX-102) and 3,4,5,6-tetrabromophthalic anhydride (SAYTEX RB-49) are miscible in HIPS and 1-bromo-4-(4-bromophenoxy)benzene is miscible in polyester. In contrast, the material 3,3',4,4',5,5',6,6'-octabromo-*N,N*-ethylenedipthalimide (SAYTEX BT-93) is harder to access by ⁸¹Br NQR; it shows only a single broad resonance in the crystalline phase. Therefore, dissolution must be deduced from change in line width and detected signal intensity. The 3,3',4,4',5,5',6,6'-octabromo-*N,N*-ethylenedipthalimide (SAYTEX BT-93)/HIPS mixture shows a reproducibly broadened resonance and loss in signal intensity, which indicates some structural change from the crystalline phase.

In the earlier study of flame retardant/HIPS mixtures by Radloff, wide-angle X-ray scattering showed a small

scattering pattern from a 12 wt % sample of 3,3',4,4',5,5',6,6'-octabromo-*N,N*-ethylenedipthalimide (SAYTEX BT-93) in HIPS, but no detectable scattering from 1-(2,3,4,5,6-pentabromophenoxy)-2,3,4,5,6-pentabromobenzene (SAYTEX-102) in HIPS. The conclusion reached on the basis of the X-ray diffraction and dynamic mechanical analysis work indicated the former is best regarded as an inert filler while the latter is miscible. The observation of a scattering pattern for 3,3',4,4',5,5',6,6'-octabromo-*N,N*-ethylenedipthalimide combined with an NQR resonance that exhibits some change on mixing with HIPS suggests a fraction of the material is dissolved in HIPS.

Chang et al. discuss the interaction of additives with a polymer matrix.³⁰ The higher the melting point of the additive in relation to the processing temperature of the plastic, the greater the chance that the additive will phase separate, creating a heterogeneous additive/polymer mixture. Consistent with Chang's result is the analysis of the NQR data presented for the three flame retardant/HIPS systems, all melt processed at 220 °C. 3,3',4,4',5,5',6,6'-octabromo-*N,N*-ethylenedipthalimide (SAYTEX BT-93; mp 450–455 °C) has a fraction phase separated from the HIPS matrix, whereas the lower melting additives 1-(2,3,4,5,6-pentabromophenoxy)-2,3,4,5,6-pentabromobenzene (SAYTEX-102; mp 304 °C) and 3,4,5,6-tetrabromophthalic anhydride (SAYTEX-RB-49; mp 276–282 °C) show no phase separation and are solubilized in the polymer.

(30) Chang, E. P.; Kirsten, R.; Slogowski *J. Appl. Polym. Sci.* **1977**, *21*, 2167–2180.

(31) Gafner, G.; Herbstein, F. H. *Acta Crystallogr.* **1960**, *13*, 706.

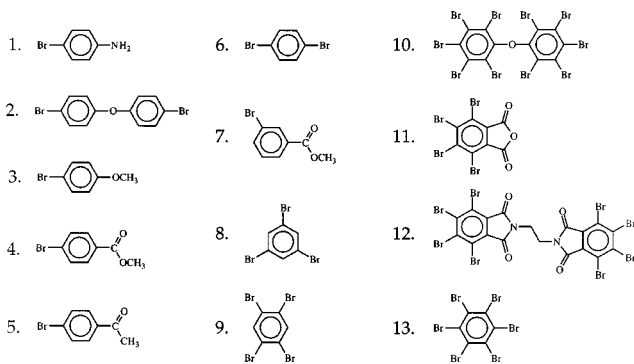
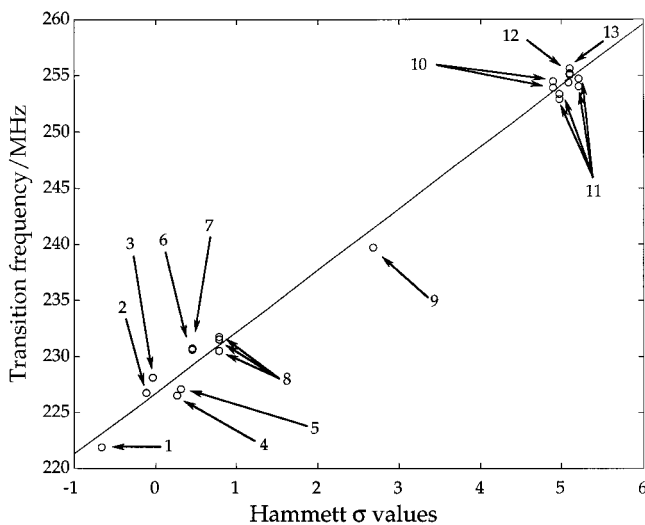


Figure 8. Correlation of ^{81}Br NQR transition frequencies with Hammett σ parameters.

Acknowledgment. The authors thank the Albe-marle Corporation for sponsoring this research and NSF

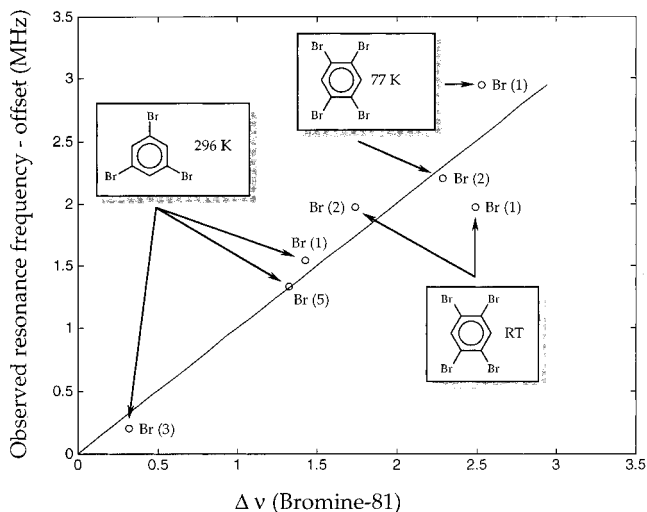


Figure 9. Correlation of ^{81}Br NQR transition frequencies with lattice effects (point charge model). Labels refer to crystallographic sites: 1,2,4,5-tetrabromobenzene at 100 K (this work), 1,2,4,5-tetrabromobenzene at room temperature,³¹ and 1,3,5-tribromobenzene at 293 K.¹⁷ The best fit to eq 7 yields $K = -0.0559$ and offsets frequencies of 230.204 MHz (1,3,5-tribromobenzene) and 239.806 MHz (1,2,4,5-tetrabromobenzene at 77 K). The offset frequency of 1,2,4,5-tetrabromobenzene at 296 K is set to 239.806 MHz, but with a correction of -2.07 MHz based on the temperature coefficient of $-3.9 \times 10^{-5}/^\circ\text{C}$.²⁶ The assignment of transition frequencies to crystallographic sites is done to achieve the best fit to the point charge model.

for funds to build the spectrometer. Improvements to the LSU X-ray Crystallography Facility were supported by Grant LEQSF(1996-97)-ENH-TR-10 administered by the Louisiana Board of Regents.

CM970541W